SUPPLEMENTARY APPENDIX

Caulobacter PopZ forms an intrinsically disordered hub in organizing bacterial cell poles

Joshua A. Holmes[1], Shelby E. Follett[2], Haibi Wang[1], Christopher Meadows[1], Krisztina Varga[2,3], and Grant R. Bowman[1]

[1] Department of Molecular Biology, University of Wyoming, Laramie WY 82071

[2] Department of Chemistry, University of Wyoming, Laramie WY 82071

[3] Current address: Department of Molecular, Cellular, and Biomedical Sciences, University of New Hampshire, Durham, NH 03824

SUPPLEMENTARY METHODS

Culture conditions and strains

C. crescentus CB15N was grown at 30°C in PYE media (0.2% bactopeptone, 0.1% yeast extract,1 mM $MgSO_4$, 0.5 mM $CaCl_2$) and imaged during log phase growth. For microscopy and BACTH experiments, *E. coli* strain BL21(DE3) was grown overnight in Luria Bertani (LB) medium, diluted 1:100, and grown to an OD_{600} of 0.3 at 37°C. To induce expression from plasmids, arabinose (0.002%-0.2%) and IPTG (10-50 μM) were added during an additional 2 hours of growth at 30°C. *E. coli* strains DH5α was used for molecular cloning. When appropriate, media were supplemented with antibiotics at the following concentrations (μg/ml in liquid/solid medium for E. coli strains); for ampicillin (50;100), chloramphenicol (20;30), kanamycin (30;50). For C. crescentus (μg/ml in liquid/solid medium); for ampicillin (5;50), chloramphenicol (1;1), kanamycin (5;25). *C. crescentus* strains CB15N was used for all experiments. When appropriate, media were supplemented with antibiotics at the following concentrations (μg/ml in liquid/solid medium); for ampicillin (10;50), kanamycin (5;25).

Plasmid construction

To create the pBAD-msfGFP entry plasmid, pBADHisA (Invitrogen) was opened with HindIII and XhoI, and a PCR product encoding msfGFP (from primers JH60 and JH67) was inserted into this site by isothermal cloning. Next, the coding sequences of PopZ binding candidate proteins were amplified using PCR, and these were inserted into pBAD-msfGFP opened with NcoI and XhoI. The ITC cloning sequences were TTGGGCTAACAGGAGGAATTAACCA for the 5' overlap and ACTGCCGCCGCCGCCGCTCTCGAG for the 3' overlap. To make the DivIVA-ParB-msfGFP fusion, DivIVA was amplified using primers JH290 and JH291, and ParB was amplified using JH288 and JH289. These two fragments were then placed into open pBAD-msfGFP by ITC.
mCherry-PopZ variants were placed into pACYC (Novagen) by opening the plasmid with NcoI and XhoI and inserting PCR-amplified variants of mCherry-PopZ by ITC. The ITC cloning sequences were 5' GTTTAACTTTAATAAGGAGATATACCATG and 3' TCGCAGCAGCGGTTTCTTTACCAGACTCGAG.
To create pBad + SpmX-msfGFP, we designed primers that would amplify the first 350 amino acids of SpmX. This produces a truncated form of SpmX that lacks the transmembrane region in amino acids 351-431, but retains PopZ-dependent polar localization in *Caulobacter* (1)(2). In all

other experiments that involved SpmX, such as the column binding assay and the bacterial 2-hybrid assay, we employed the same truncated form of the protein (aa 1-350). To make pBad + SpmX-msfGFP we used the following ITC cloning primers: 5' primer CGCGAACAGATTGGAGGTatgaaaccgcgtcatcag 3' GTGGCGGCCGCTCTATTAcagatcatcctggcgc, capital letters denote overlap with pETITE vector, lowercase letters are overlap with SpmX.
The bacterial two-hybrid assay plasmids pUT18 and pKT25 (Euromedex) were modified as follows. For candidate PopZ binding proteins, pUT18 was opened with HindIII and EcoRI, and candidate protein coding sequences were amplified by PCR and inserted into the open plasmid by ITC. The ITC cloning sequences were 5' CTATGACCATGATTACGCCAAGCTT and 3' CGTGGCCTCGCTGGCGGCTGAATTC. To place PopZ variants into pKT25, the plasmid was opened with PstI and EcoRI, and PCR amplified popZ variants were inserted by ITC. The ITC cloning sequences were 5' CTGGCGCGCACGCGGCGGGCTGCAG and 3' ACGTTGTAAAACGACGGCCGAATTC.
To create a *Caulobacter* strain expressing McpA-GFP, the McpA coding sequence was fused to the coding sequence for GFP, and the combined sequence was cloned into plasmid pVMCS4. Following electroporative transformation, the plasmid inserted into the *Caulobacter* chromosome by homologous recombination at the P_{vanA} promoter (3). Due to the low level of constitutive expression and the high stability of McpA-GFP, the addition of vanillate inducer was not necessary for obtaining a visible fluorescent signal.
To create a *Caulobacter* strain expressing mCherry-PopZ, the mCherry-PopZ coding sequence was cloned into the plasmid pBXMCS-4, enabling plasmid-based expression from the $P_{van}A$ promoter in *Caulobacter* cells (3). Due to the low level of constitutive expression and the high stability of mCherry-PopZ, the addition of vanillate inducer was not necessary for obtaining a visible fluorescent signal.
Strains using CckA-CFP and PopZ truncations were made using a PopZ KO strain with CckA-CFP integrated into the chromosome JH442. pBXMCS-2 was digested using NdeI and SacI, this was combined by PCR fragments of various PopZ truncations and via ITC combined. The plasmids were then introduced into JH442 via electroporative transformation.
Plasmid creation for in-vitro pull down assay. For SpmX-his tagged protein a commercial kit (Lucigen) was used. SpmX was PCR amplified and combined with commercial pre-processed pETite vector transformed directly into competent HI-Control 10G cells (Lucigen). For Strep tagged PopZ pASK-IB3+ plasmid was digested using NcoI and XhoI. PCR amplified popZ was inserted by ITC.

PopZ PED protein sequences
To create various PED linkers ITC was done by combining mCherry-PopZ n-terminal with C-term PopZ and pACYC backbone. pACYC plasmid was prepared by digesting with NcoI and BalI enzymes. 5' primer for all constructs mCherry-PopZ n-terminal fragments was TAACTTTAATAAGGAGATATACCATGGatgagcaagggcgag capital letters denote pACYC overlap and lowercase is mCherry. 3' for all constructs of C-terminal PopZ-pACYC overlap was CACCAGTTTTGATTTAAACGTGGCCatatggacaacttcttc, uppercase is pACYC overlap with vector and lowercase is pACYC fragment amplified with c-terminal PopZ**.**
Univerisal 5' mCherry primer was used with 3' primer CGGCGCCGCCGCATCCGCCGGCGGCGGATCTTCTTCctccgagatgatgcgt was used to create first half

of the scrambled PED linker; EEDPPPADAAAPPAPEAVPPEPPE and 5’ CCGGCGCCGGAAGCGGTGCCGCCGGAACCGCCGGAAcggacgctggaagacg was used with univerisal 3’ c-term pACYC primer to create second half.
Univerisal 5’ mCherry primer was used with 3’ primer GCTCGCCGCCGCATCCGCGCTGCTGCTATCGCCGCCctccgagatgatgcgt to create first half of GS PED linker; GGDSSSADAAASSASGAVSSGSSG and 5’ GCCGCTGCTGCCGCTGCTCACCGCGCCGCTCGCGCTcggacgctggaagacg was used with univerisal 3’ c-term pACYC primer to create second half.
Univerisal 5’ mCherry primer was used with 3’ primerCGCCGCCGGCGCCGCCGGCGGCGCCGGCGCCGGCGGctccgagatgatgcgt was used to create first half of the Proline PED linker; PPAPAPPAAPAAPPPPPPPPAAP and 5’ CGCCGCCGGCGCCGCCGGCGGCGCCGGCGCCGGCGGcggacgctggaagacg was used with univerisal 3’ c-term pACYC primer to create second half.
Univerisal 5’ mCherry primer was used with 3’ primer CGGCGCCGCCGCATCCGCCGGCGGCGGATCTTCTTCctccgagatgatgcgt was used to create first half of the ½ Scrambled PED linke; EEDPPPADAAAP and 5’ GAAGAAGATCCGCCGCCGGCGGATGCGGCGGCGCCGcggacgctggaagacg was used with univerisal 3’ c-term pACYC primer to create second half.

Widefield Fluorescence Microscopy
Cells were immobilized on a 1% agarose pad containing LB media for *E. coli* cells and M2G for *C. crescentus*. Live-cell imaging was performed using a Zeiss Axio Imager Z2 epifluorescence microscope equipped with a Hamamatsu Orca-Flash4.0 sCMOS camera and a Plan-Apochromat 100x/1.46 Oil Ph3 objective. Zeiss Filter sets 47HE, 38HE, 46HE, and 63HE were used to acquire fluorescent images of CFP, msfGFP, eYFP and mCherry, respectively. Images were collected and processed with Zen Blue software.

Fluorescent Image Analysis
Fluorescent microscopy images were analyzed via the MicrobeTracker (4) suite running on MATLAB 2015b. E. *coli* cell meshes were obtained using MicrobeTracker algorithm 4. The MATLAB graythresh method was used to determine a threshold for fluorescence localization within the cell meshes. Percent localization was then calculated as the sum of the fluorescent signal which exceeded the threshold for background fluorescence divided by the sum of the fluorescent signal within each cell mesh.

Bacterial 2-hybrid assay
The Euromedex BACTH Bacterial Adenylate Cyclase Two-Hybrid System Kit was used with assay methods developed by Park and Jiao (5). Two negative controls were utilized: *E. coli* lacking CyaA components (CyaA null) and CyaA T25-PopZ with GFP-CyaA T18. To test for protein interaction, CyaA T25-PopZ variants were tested with candidate proteins expressed as N-terminal fusions to CyaA T18. All experiments were performed in a cyaA mutant background.

***In vitro* column binding assay**

6His-Sumo-tagged proteins were expressed in *E. coli* strain BL21 Rosetta (EMD Millipore), purified under native conditions by cobalt affinity chromatography (Thermo), and eluted in buffer HMK (20mM HEPES pH 7.5, 2 mM MgCl2, 100 mM KCl) + 250 mM imidazole. The PopZ affinity column was prepared by expressing PopZ-streptag in *E. coli* strain DH5α, passing the clarified lysate through a 0.2ml bed volume column containing Streptacin XL resin (IBA Life Sciences), and washing in buffer HMK. Lysates were prepared in by pulsed sonication (Branson). His-tagged protein samples were diluted 4-fold in Buffer HMK, passed through the PopZ affinity column, washed twice with 0.8 ml of buffer, and eluted with biotin.

Fluorescence loss in photobleaching (FLIP) assays

FLIP experiments were performed using confocal illumination, provided by an LMM5 laser launch (Spectral Applied research). Integration of all imaging systems components was provided by Biovision Technologies (Exton, PA). All image acquisition and analysis was performed using Metamorph 7.7 software (Molecular Devices). Images were acquired using Olympus objective 60 x/1.49 Oil DIC. ILAS^2 equipment was used to control laser power (at 10%) and position.

PopZ Purification for NMR experiments

The PopZΔ134-177 coding sequence was inserted into plasmid pET28a (Novagen) at the NcoI and XhoI restriction sites and transformed into Novagen® RosettaTM (Novagen). To express the 6xHis-tagged protein, a stationary culture was diluted 1:100-1:200 into 2 l fresh LB medium and grown at 37 °C with shaking at 200 rpm. At OD600 of 0.4, the cells were spun down at 7,700 × *g* for 15 minutes at 4 °C, resuspended in ¼ volume of M9 media (48 mM Na_2HPO_4, 22 mM KH_2PO_4, 9 mM NaCl, 2 mM $MgSO_4$, 0.1 mM $CaCl_2$, 0.4% ^{13}C-glucose, 18 mM $^{15}NH_4Cl$ with kanamycin at 30 µg/mL and chloramphenicol at 20 µg/mL), and incubated overnight with 0.8 mM IPTG and shaking at 200 rpm. $^{15}NH_4Cl$ was purchased from Cambridge Isotope Laboratories, Inc. Frozen cell pellets were resuspended with ice cold binding buffer (25 mM Tris, 150 mM NaCl, 20 mM imidazole at pH 7.5) supplemented with EDTA free protease inhibitor and Benzonase nuclease. Cells were lysed using a French press, and the cell debris was removed by centrifugation (20 minutes at 27,200 ×g and 4 °C). The supernatant was filtered through a 0.22 µm syringe filter (Millipore) and concentrated. The protein was purified using a Fast Protein Liquid Chromatography instrument (FPLC; GE Healthcare ÄKTA purifier 900) equipped with a Ni-NTA column (GE Healthcare HisTrap HP 1 ml column). The sample was loaded onto the Ni-NTA column pre-equilibrated with binding buffer, washed, and eluted in the same buffer with a gradient of up to 500 mM imidazole. The peak protein-containing fractions were then re-loaded onto an Ni-NTA column for an additional round of washing and elution. This was repeated for a total of three rounds of Ni-NTA purification. Peak fractions were pooled and dialyzed in 25 mM Tris, 150 mM NaCl pH 7.5 for 2 hours, then switched to fresh buffer and dialyzed overnight. The purity of the sample was analyzed by 12.5% SDS-PAGE and staining with Coomassie blue.

High Field NMR spectroscopy

For High field NMR experiments, the purified popZ was buffer exchanged into a citrate-phosphate buffer (50 mM phosphate, 50 mM citric acid, 20 mM NaCl, and 3 mM NaN_3 at pH 5.5). The sample was concentrated to 300 µL for NMR experiments, and D2O, NaN3, and DSS were added to a 10% v/v, 4 mM and 1 mM final concentration, respectively. The concentration was estimated as 420 µM using UV-Visible spectrophotometry (ε280 =2,980 cm-1M-1). The NMR sample was packed into a Shigemi NMR tube. The ^{1}H-^{15}N HSQC (Heteronuclear Single Quantum Correlation) NMR spectrum was collected at 25 °C on a VNMRS 800-MHz spectrometer equipped with and HCN z-axis gradient cold probe.

Circular Dichroism

$PopZ^{\Delta 134-177}$ was purified as described for NMR and exchanged into 20 mM Na_2HPO_4 pH 7.5 at a final concentration of 18µM. The sample was analyzed in an Aviv 430 spetropolarimeter equipped with Peltier temperature control.

Purification of RcdA, ChpT, and His-SUMO-DivK for NMR

The coding sequences of *rcdA* and *chpT* were amplified by PCR and co-transformed into Lucigen HI-Control™ 10G cells with pETite™ N-His SUMO. The resulting plasmids were transformed into Lucigen HI-Control™ BL21(DE3), generating strains HW#293/294. To express protein, cultures were grown at 37°C in LB until OD_{600nm} 0.5, and induced overnight with 1mM IPTG at 21°C with shaking at 200rpm. Frozen cell pellets were resuspended with ice cold binding buffer (20 mM HEPES, 100 mM KCl, 2 mM $MgCl_2$, 20 mM imidazole at pH 7.5 adjusted with KOH) supplemented with EDTA free protease inhibitor and Benzonase nuclease. Cells were lysed using a French press, and the cell debris was removed by centrifugation (20 minutes at 27,200 × *g* and 4 °C). The supernatant was filtered through a 0.22 µm syringe filter (Millipore) and concentrated. The protein was purified using a Fast Protein Liquid Chromatography instrument (FPLC; GE Healthcare ÄKTA purifier 900) equipped with a Ni-NTA column (GE Healthcare HisTrap HP 1 ml column). The sample was loaded onto the Ni-NTA column pre-equilibrated with binding buffer, washed, and eluted in the same buffer with a gradient of up to 500 mM imidazole. The peak protein-containing fractions were then re-loaded onto a Ni-NTA column for an additional round of washing and elution after removing high concentration of imidazole. The purity of the samples were analyzed by 12.5% SDS-PAGE and staining with Coomassie blue.

His-SUMO-DivK was buffer exchanged (Zeba spin desalting columns 7K MWCO, 5 mL) to 20 mM HEPES, 100 mM KCl, 2 mM $MgCl_2$ at pH 7.5 (adjusted with KOH) for NMR experiments.

After the initial 2 step purification, RcdA and ChpT were buffer exchanged to 25 mM Tris, 150 mM NaCl pH 7.5 buffer and diluted to approximately 1mg/mL concentration. SUMO Express Protease (Lucigen) was then added at a concentration of 1 unit per 50-100 µg protein, along with 2 mM final concentration of fresh DTT. Digests were incubated at 4°C overnight, followed by additional incubation at 30°C for another day after the addition of 1 mM fresh DTT.

After cleavage, the proteins were passed through an additional Ni-NTA column and the flow through was collected. The flow through contained the cleaved proteins which were buffer exchanged to 20 mM HEPES, 100 mM KCl, 2 mM $MgCl_2$ at pH 7.5 (adjusted with KOH) for NMR experiments. The purity of the samples were analyzed by 12.5% SDS-PAGE and staining with Coomassie blue.

NMR sample conditions for testing protein interactions

For NMR experiments, the purified PopZ was buffer exchanged into 20 mM HEPES, 100 mM KCl, 2 mM $MgCl_2$ at pH 7.5 (adjusted with KOH). The concentration for each sample was estimated using UV-Visible spectrophotometry and final concentrations were calculated (see table below). Each sample was prepared by mixing PopZ with one of the binding partners (in the necessary volumes needed to obtain the final concentrations) and then concentrating to 300 µL. For NMR experiments D_2O, NaN_3 and DSS were added to a 10% v/v, 1 mM and 1 mM final concentration, respectively. The NMR sample was packed into a Shigemi NMR tube. The 2D ^{1}H-^{15}N HSQC (Heteronuclear Single Quantum Correlation) NMR spectra were collected at 25 °C on a Bruker 600 MHz spectrometer equipped with a 5 mm SmartProbe™.

Sample #	[PopZ] (µM) (ε_{280} =2,980 $cm^{-1}M^{-1}$)	Binding Partner	[Binding Partner] (µM)
1	146	-	-
2	146	RcdA (ε_{280} = 18,450 $cm^{-1}M^{-1}$)	1150
3	146	ChpT (ε_{280} = 17,990 $cm^{-1}M^{-1}$)	614
4	157	DivK (ε_{280} = 9,970 $cm^{-1}M^{-1}$)	596
5	157	DivK (ε_{280} = 9,970 $cm^{-1}M^{-1}$) RcdA (ε_{280} = 18,450 $cm^{-1}M^{-1}$)	596 442
6	157	BSA (ε_{280} = 43,824 $cm^{-1}M^{-1}$)	416

E. coli strains

Strain	pBAD	pACYC	pKT25	pUT18c	Other	Source
JH42		*mcherry-popZ*				This study
JH50	*divK-msfgfp*	*mcherry-popZ*				This study
JH51	*pleC-msfgfp*	*mcherry-popZ*				This study
JH58	*clpX-msfgfp*	*mcherry-popZ*				This study
JH61	*cckA-msfgfp*	*mcherry-popZ*				This study
JH64	*rcdA-msfgfp*	*mcherry-popZ*				This study
JH66	*msfgfp*					This study
JH68	*msfgfp*	*mcherry-popZ*				This study
JH76	*divJ-msfgfp*	*mcherry-popZ*				This study
JH77	*mipZ-msfgfp*	*mcherry-popZ*				This study
JH78	*podJ-msfgfp*	*mcherry-popZ*				This study
JH79	*divL-msfgfp*	*mcherry-popZ*				This study
JH80	*staR-msfgfp*	*mcherry-popZ*				This study
JH81	*parB-msfgfp*	*mcherry-popZ*				This study
JH86	*cpdR-msfgfp*	*mcherry-popZ*				This study
JH87	*pdeA-msfgfp*	*mcherry-popZ*				This study
JH88	*pleD-msfgfp*	*mcherry-popZ*				This study
JH89	*tipR-msfgfp*	*mcherry-popZ*				This study
JH93	*popA-msfgfp*	*mcherry-popZ*				This study
JH98	*ctrA-msfgfp*	*mcherry-popZ*				This study
JH100		*icsA*$^{\Delta 1\text{-}506+\Delta 621\text{-}1102}$*-mcherry*				This study
JH113	*dlvL*$^{\Delta 1\text{-}138}$*-msfgfp*	*mcherry-popZ*				This study
JH114	*clpP-msfgfp*	*mcherry-popZ*				This study
JH135	*cckA*$^{\Delta 1\text{-}72}$*-msfgfp*	*mcherry-popZ*				This study
JH136	*dnaK-msfgfp*	*mcherry-popZ*				This study
JH148	*dgcB-msfgfp*	*mcherry-popZ*				This study
JH154	*cc_3225-msfgfp*	*mcherry-popZ*				This study
JH155	*chpT-msfgfp*	*mcherry-popZ*				This study
JH179	*popZ-msfgfp*					This study
JH205	*dlvL*$^{\Delta 1\text{-}138\ \Delta 723\text{-}769}$*msfgfp*	*mcherry-popZ*				This study
JH207	*dlvL*$^{\Delta 723\text{-}769}$*msfgfp*	*mcherry-popZ*				This study
JH206	*parB-msfgfp*	*mcherry-popZ*$^{\Delta n\text{-}term}$				This study
JH207	*dlvL*$^{\Delta 1\text{-}138}$*-msfgfp*	*mcherry-popZ*$^{\Delta n\text{-}term}$				This study
JH208	*cckA-msfgfp*	*mcherry-popZ*$^{\Delta n\text{-}term}$				This study
JH209	*parB-msfgfp*	*mcherry-popZ*$^{\Delta ped}$				This study
JH209	*parB-msfgfp*	*mcherry-popZ*$^{\Delta 24\text{-}81}$				This study
JH210	*rcdA-msfgfp*	*mcherry-popZ*$^{\Delta 24\text{-}81}$				This study
JH211	*cpdR-msfgfp*	*mcherry-popZ*$^{\Delta 24\text{-}81}$				This study
JH212	*chpT-msfgfp*	*mcherry-popZ*$^{\Delta 24\text{-}81}$				This study
JH213	*dlvL*$^{\Delta 1\text{-}138}$*-msfgfp*	*mcherry-popZ*$^{\Delta 24\text{-}81}$				This study

JH214	*parB-msfgfp*	*mcherry-popZ*$^{\Delta 24\text{-}81}$	This study
JH215	*parB-msfgfp*	*mcherry-popZ*$^{\Delta 48\text{-}102}$	This study
JH226	*parB-msfgfp*	*divIVA-mcherry-popZ*	This study
JH227	*cckA-msfgfp*	*mcherry-popZ*$^{\Delta 24\text{-}81}$	This study
JH229	*parB-msfgfp*	*mcherry-popZ*$^{\Delta 134\text{-}177}$	This study
JH237	*chpT-msfgfp*	*mcherry-popZ*$^{\Delta n\text{-}term}$	This study
JH241	*grcA-msfgfp*	*mcherry-popZ*	This study
JH242	*vanA-msfgfp*	*mcherry-popZ*	This study
JH252	*Spmx-msfgfp*$^{\Delta 351\text{-}431}$	*mcherry-popZ*	This study
JH253	*rcdA-msfgfp*	*mcherry-popZ*$^{\Delta n\text{-}term}$	This study
JH254	*cpdR-msfgfp*	*mcherry-popZ*$^{\Delta n\text{-}term}$	This study
JH260	*Spmx-msfgfp*$^{\Delta 351\text{-}431}$	*mcherry-popZ*$^{\Delta 24\text{-}81}$	This study
JH262	*parB-msfgfp*	*mcherry-popZ*$^{\Delta h2}$	This study
JH266	*parB-msfgfp*	*divIVA-mcherry-popZ*$^{\Delta 124\text{-}177}$	This study
JH266	*dlvL*$^{\Delta 1\text{-}138}$*-msfgfp*	*mcherry-popZ*$^{\Delta h2}$	This study
JH267	*Spmx-msfgfp*$^{\Delta 351\text{-}431}$	*mcherry-popZ*$^{\Delta n\text{-}term}$	This study
JH274	*rcdA-msfgfp*	*mcherry-popZ*$^{\Delta h2}$	This study
JH275	*cckA-msfgfp*	*divIVA-mcherry-popZ*$^{\Delta 124\text{-}177}$	This study
JH276	*cpdR-msfgfp*	*mcherry-popZ*$^{\Delta h2}$	This study
JH278	*chpT-msfgfp*	*divIVA-mcherry-popZ*$^{\Delta 124\text{-}177}$	This study
JH279	*cpdR-msfgfp*	*divIVA-mcherry-popZ*$^{\Delta 124\text{-}177}$	This study
JH280	*rcdA-msfgfp*	*divIVA-mcherry-popZ*$^{\Delta 124\text{-}177}$	This study
JH281	*Spmx-msfgfp*$^{\Delta 351\text{-}431}$	*divIVA-mcherry-popZ*$^{\Delta 124\text{-}177}$	This study
JH282	*dlvL*$^{\Delta 1\text{-}138}$*-msfgfp*	*divIVA-mcherry-popZ*$^{\Delta 124\text{-}177}$	This study
JH283	*parB-msfgfp*	*divIVA-mcherry-popZ*$^{\Delta 134\text{-}177}$	This study
JH284	*cckA-msfgfp*	*divIVA-mcherry-popZ*$^{\Delta 134\text{-}177}$	This study
JH285	*chpT-msfgfp*	*divIVA-mcherry-popZ*$^{\Delta 134\text{-}177}$	This study
JH286	*cpdR-msfgfp*	*divIVA-mcherry-popZ*$^{\Delta 134\text{-}177}$	This study
JH287	*rcdA-msfgfp*	*divIVA-mcherry-popZ*$^{\Delta 134\text{-}177}$	This study
JH288	*Spmx-msfgfp*$^{\Delta 351\text{-}431}$	*divIVA-mcherry-popZ*$^{\Delta 134\text{-}177}$	This study
JH289	*dlvL*$^{\Delta 1\text{-}138}$*-msfgfp*	*divIVA-mcherry-popZ*$^{\Delta 134\text{-}177}$	This study
JH301	*chpT-msfgfp*	*mcherry-popZ*$^{\Delta 48\text{-}102}$	This study
JH302	*cckA-msfgfp*	*mcherry-popZ*$^{\Delta 48\text{-}102}$	This study
JH303	*rcdA-msfgfp*	*mcherry-popZ*$^{\Delta 48\text{-}102}$	This study
JH304	*parB-msfgfp*	*mcherry-popZ*$^{\Delta 48\text{-}102}$	This study
JH305	*cpdR-msfgfp*	*mcherry-popZ*$^{\Delta 48\text{-}102}$	This study
JH306	*dlvL*$^{\Delta 1\text{-}138}$*-msfgfp*	*mcherry-popZ*$^{\Delta 48\text{-}102}$	This study
JH307	*Spmx-msfgfp*$^{\Delta 351\text{-}431}$	*mcherry-popZ*$^{\Delta 48\text{-}102}$	This study
JH321	*cckA-msfgfp*	*mcherry-popZ*$^{\Delta h2}$	This study
JH322	*chpT-msfgfp*	*mcherry-popZ*$^{\Delta h2}$	This study
JH323	*chpT-msfgfp*	*mcherry-popZ*$^{\Delta ped}$	This study
JH324	*cpdR-msfgfp*	*mcherry-popZ*$^{\Delta ped}$	This study
JH325	*rcdA-msfgfp*	*mcherry-popZ*$^{\Delta ped}$	This study

JH326	*Spmx-msfgfp*$^{\Delta 351-431}$	*mcherry-popZ*$^{\Delta ped}$				This study
JH327	*dIvIL*$^{\Delta 1-138}$*-msfgfp*	*mcherry-popZ*$^{\Delta ped}$				This study
JH328	*cckA-msfgfp*	*mcherry-popZ*$^{\Delta ped}$				This study
JH337			*cyaA-T25-popZ*	*parB-cyaA-T18*		This study
JH340			*cyaA-T25-popZ*$^{\Delta 134-177}$	*parB-cyaA-T18*		This study
JH343			*cyaA-T25-popZ*	*msfgfp-cyaA-T18*		This study
JH344			*cyaA-T25-popZ*$^{\Delta 134-177}$	*msfgfp-cyaA-T18*		This study
JH356			*cyaA-T25-popZ*	*cckA-cyaA-T18*		This study
JH357			*cyaA-T25-popZ*	*cckA*$^{\Delta 1-72}$*-cyaA-T18*		This study
JH365			*cyaA-T25-popZ*	*Spmx*$^{\Delta 351-431}$*cyaA-T18*		This study
JH366			*cyaA-T25-popZ*	*cpdR-cyaA-T18*		This study
JH367			*cyaA-T25-popZ*	*rcdA-cyca-T18*		This study
JH368			*cyaA-T25-popZ*	*chpT-cyaA-T18*		This study
JH369			*cyaA-T25-popZ*	*dIvL* $^{\Delta 1-138}$*-T18*		This study
JH373	*tipN-msfgfp*	*mcherry-popZ*				This study
JH374	*divIVA-parB-msfgfp*	*mcherry-popZ*$^{\Delta 134-177}$				This study
JH375	*Spmx-msfgfp*$^{\Delta 351-431}$	*mcherry-popZ*$^{\Delta h2}$				This study
JH387			*cyaA-T25-popZ*$^{\Delta 134-177}$	*dIvL*$^{\Delta 1-138}$*-T18*		This study
JH388			*cyaA-T25- popZ*$^{\Delta 134-177}$	*rcdA-cyca-T18*		This study
JH389			*cyaA-T25- popZ*$^{\Delta 134-177}$	*cpdR-cyaA-T18*		This study
JH390			*cyaA-T25- popZ*$^{\Delta 134-177}$	*chpT-cyaA-T18*		This study
JH391			*cyaA-T25- popZ*$^{\Delta 134-177}$	*Spmx*$^{\Delta 351-431}$*cyaA-T18*		This study
JH392			*cyaA-T25- popZ*$^{\Delta 134-177}$	*cckA-cyaA-T18*		This study
JH414	*parB-msfgfp*	*mcherry-popZ*$^{\Delta \text{ PED:scr linker}}$				This study
JH415	*parB-msfgfp*	*mcherry-popZ*$^{\Delta \text{ PED:gs linker}}$				This study
JH416	*parB-msfgfp*	*mcherry-popZ*$^{\Delta \text{ PED:proline linker}}$				This study
JH417	*parB-msfgfp*	*mcherry-popZ*$^{\Delta \text{ PED:1/2 scr linker}}$				This study
JH425	*parB-msfgfp*	*divIVA-mcherry-popZ*$^{\Delta PED;\ \Delta 134-177}$				This study
JH470					*popZ* in pASK-IBA3+	This study
JH472					*Spmx*$^{\Delta 351-431}$ in pETite	This study
HW293					*rcdA in pETite*	This study
HW294					*chpT in pETite*	This study

Caulobacter strains

Strain	Description	Source
GB050	*vanA :: pVanA – mcpA-gfp*	This study
LS3310	*cckA :: cckA-gfp*	(6)
GB438	pBXMCS4 + *mCherry-popZ*	(3)
JH443	*mVenus-popZ* in pBXMCS-2, *cckA :: ccka-cfp*	This study
JH444	*mVenus-popZ*$^{\Delta 24\text{-}81}$ in pBXMCS-2, *cckA :: ccka-cfp*	This study
JH445	*mVenus-popZ*$^{\Delta 48\text{-}102}$ in pBXMCS-2, *cckA :: ccka-cfp*	This study
JH446	*mVenus-popZ*$^{\Delta n\text{-}term}$ in pBXMCS-2, *cckA :: ccka-cfp*	This study
JH447	*mVenus-popZ*$^{\Delta h2}$ in pBXMCS-2, *cckA :: ccka-cfp*	This study
JH448	*mVenus-popZ*$^{\Delta PED}$ in pBXMCS-2, *cckA :: ccka-cfp*	This study

CCNA	Protein	Description	Localization (without mCherry PopZ)	Localization (with co-expressed mCherry PopZ)
CCNA_00010	DnaK	Polar/Midline	Foci	Partial co-localization
CCNA_00781	CpdR	Polar/Cell cycle	Diffuse	Co-localized
CCNA_00852	TipR	Polar/Cell cycle	Diffuse	Diffuse
CCNA_00852	ClpP	Polar/Cell cycle	Diffuse	Diffuse
CCNA_01116	DivJ	Polar/Cell cycle	Diffuse	Diffuse
CCNA_01132	CckA	Polar/Cell cycle	Diffuse	Co-localized
CCNA_01552	TipN	Polar/Cell cycle	Foci	Partial co-localization
CCNA_01918	PopA	Polar/Cell cycle	Foci	Partial co-localization
CCNA_01926	DgcB	Polar/Cell cycle	Diffuse	Diffuse
CCNA_02039	ClpX	Polar/Cell cycle	Diffuse	Diffuse
CCNA_02125	PodJ	Polar/Cell cycle	Foci	Non-overlapping foci
CCNA_02246	MipZ	Polar/Cell cycle	Diffuse	Diffuse
CCNA_02255	SpmX	Polar/Cell cycle	Diffuse	Co-localized
CCNA_02328	GcrA	Cell cycle	Diffuse	Diffuse
CCNA_02334	StaR	Polar/Cell cycle	Diffuse	Diffuse
CCNA_02476	VanA	Cytoplasmic	Diffuse	Diffuse
CCNA_02546	PleD	Polar/Cell cycle	Foci	Partial co-localization
CCNA_02547	DivK	Polar/Cell cycle	Diffuse	Diffuse
CCNA_02567	PleC	Polar/Cell cycle	Diffuse	Diffuse
CCNA_03130	CtrA	Polar/Cell cycle	Diffuse	Diffuse
CCNA_03333	CC_3225	Polar	Foci	Non-overlapping foci
CCNA_03404	RcdA	Polar/Cell cycle	Diffuse	Co-localized
CCNA_03507	PdeA	Polar	Diffuse	Partial co-localization
CCNA_03584	ChpT	Cell cycle	Diffuse	Co-localized
CCNA_03598	DivL	Polar/Cell cycle	Diffuse	Co-localized
CCNA_03868	ParB	Polar/Cell cycle	Diffuse	Co-localized

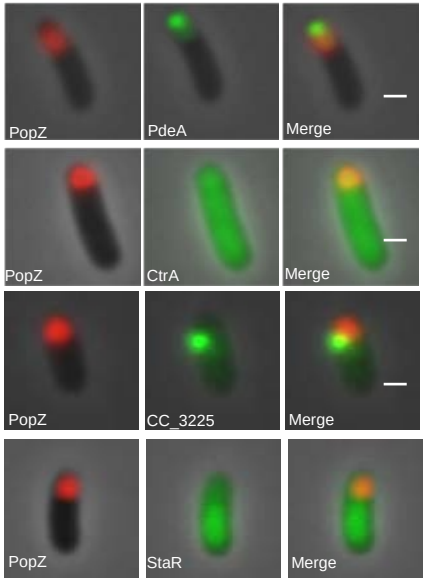

Supplementary Figure S1: Candidate proteins use in *E. coli* co-expression assay (Table, left). Examples of GFP-tagged candidate proteins co-expressed with mCherry-PopZ (Right panels). PdeA shows partial co-localization, CC_3225 shows non-overlapping foci, and CtrA and StaR are two examples of diffuse signals. StaR and some other proteins appeared to be partly excluded from PopZ foci. Fluorescence signals (red and green) are overlayed on the phase contrast image (grayscale).

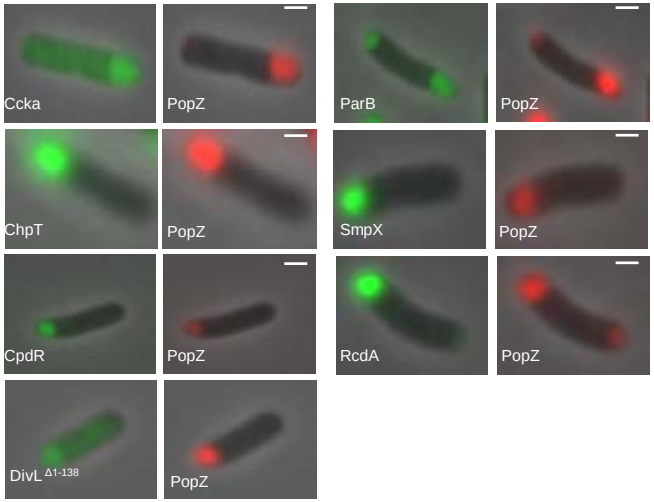

Supplementary Figure S2: Candidate proteins that exhibit co-localization with PopZ in the E. *coli* co-expression assay. GFP-tagged candidate proteins are co-expressed with mCherry-PopZ. Fluorescence signals (red and green) are overlayed on the phase contrast image (grayscale).

	CckA	ChpT	CpdR	DivL$^{\Delta 1\text{-}138}$	ParB	RcdA	SpmX
WT PopZ	10.2	43.6	15.2	19.4	26.5	16.6	15.7
PopZ ΔPED	Nd	Nd	Nd	Nd	Nd	Nd	Nd
PopZ ΔN-term	Nd	Nd	Nd	Nd	Nd	Nd	Nd
PopZ Δ48-102	8.9	40.2	13.8	17.4	23.2	14.1	13.8
PopZ Δ24-81	8.1	41.4	14.3	17.3	24.2	14.7	14.2
PopZ ΔH2	Nd	Nd	Nd	Nd	Nd	Nd	Nd
DiviVA-PopZ Δ134-177	7.3	39.1	12.7	16.3	22.5	11.2	12.1
DiviVA-PopZ Δ124-177	Nd	Nd	Nd	Nd	Nd	Nd	Nd

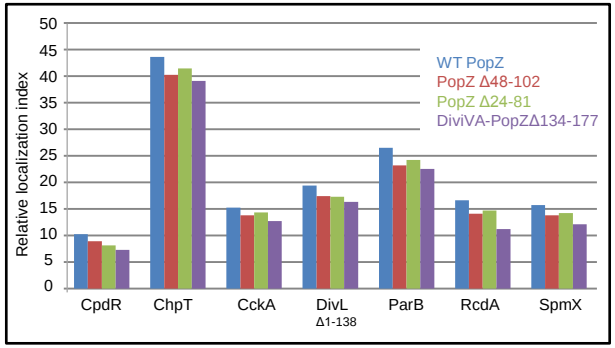

Supplementary Figure S3: Analysis of PopZ interactions using automated computational methods. (Top Panel): Measurement of the co-localization between GFP-tagged candidate binding proteins and variants of mCherry-tagged PopZ, using automated image quantitation. A minimum of 1000 cells was used for each data point, and the standard deviation for all reported values is less than 0.18 (not shown). Values under 2% were not discernable by eye and are reported as not detectable (ND). (Lower Panel): A graphical representation of the values reported in the upper panel. Notably, each of the mutations in PopZ affected interactions with all candidate binding partners to a roughly equivalent degree.

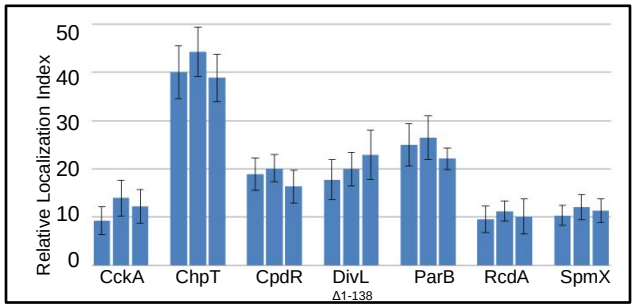

Supplementary Figure S4. The E. *coli* co-localization screen produces consistent results. The polar recruitment of GFP-tagged candidate proteins was assessed in three separate experiments, and the relative localization index was measured as described in the methods section of the main text. Error bars represent the standard deviation.

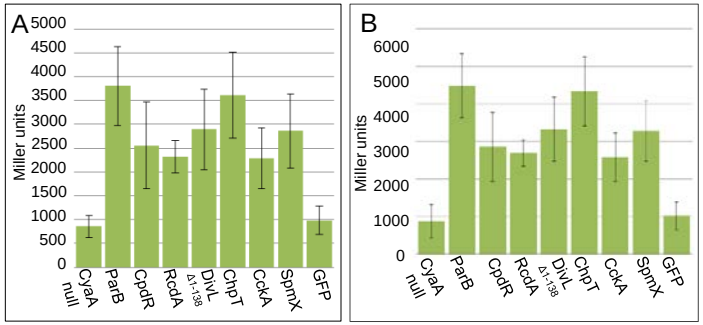

Supplementary Figure S5. A bacterial two-hybrid assay for assessing interactions between PopZ and candidate proteins. (A) Full length PopZ tested against positive candidates from the *E. coli* co-expression assay, with CyAnull and GFP as negative controls. (B) PopZ$^{\Delta 134\text{-}177}$, a monomeric variant of PopZ with diffuse localization, tested against the same candidates as in A.

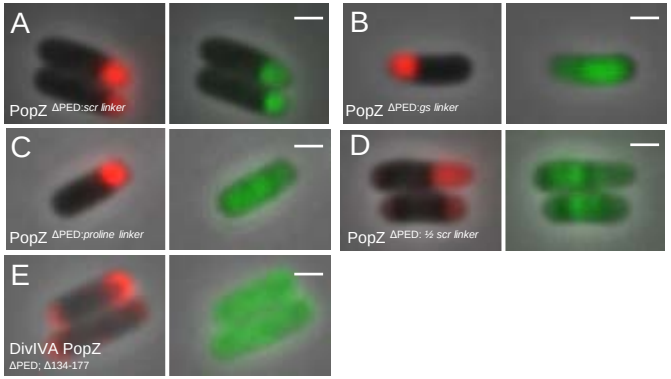

Supplementary Figure S6: Testing PopZ variants with mutations in the PED region in the *E. coli* co-expression assay. (A) The PED region was replaced with a scrambled sequence of amino acids from 24-47 (B) The PED region was replaced with a 24 amino acid gly/ser linker. (C) The PED region was replaced with 24 amino acid pro/ser linker. (D) The PED region was replaced with 12 amino acids from the insert in A. (E) DivIVA was fused with N-N-term of PopZ (1-23) and H2 (103-133). In all panels, the GFP-labeled protein is ParB-GFP. Fluorescence signals (red and green) are overlayed on the phase contrast image (grayscale).

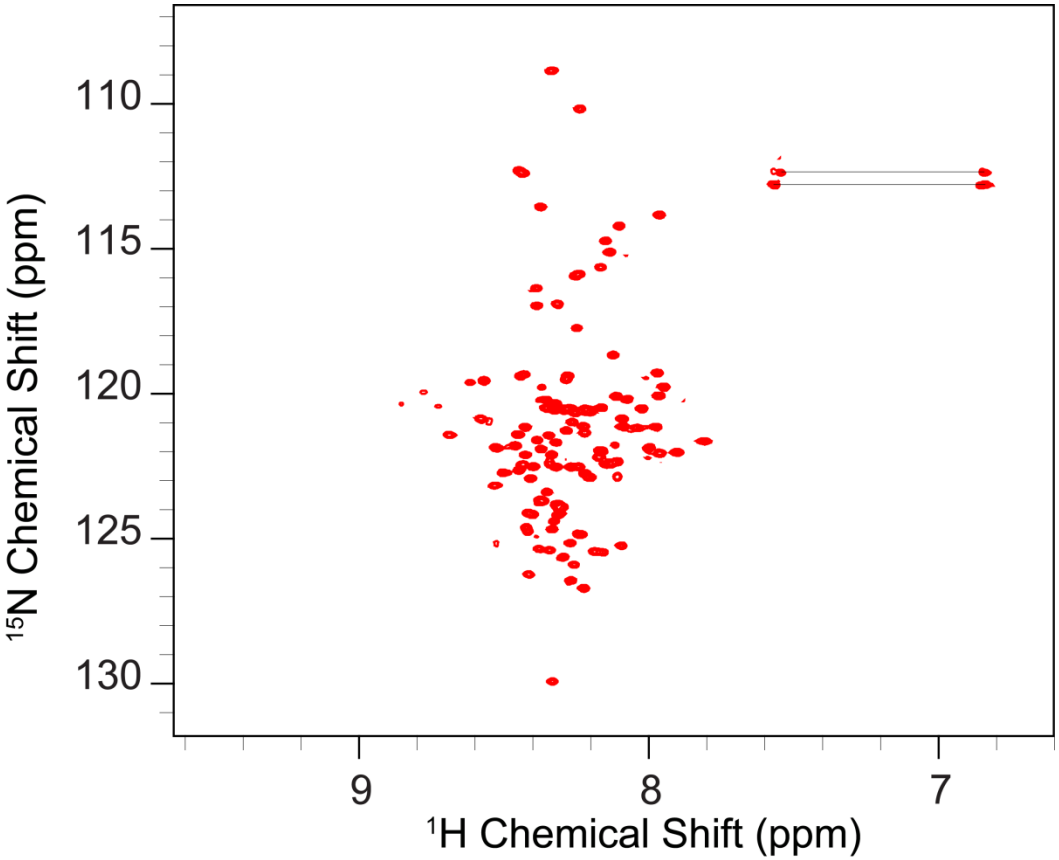

Supplementary Figure S7. 2D ^{1}H-^{15}N HSQC NMR spectrum of PopZ$^{\Delta 134\text{-}177}$, collected on a high field 800 MHz NMR spectrometer at 25 °C. The data shows well-defined peaks with roughly uniform intensities and line shapes for the majority of resonances. All of the backbone proton peaks were clustered in the 7.80-8.85 ppm region. This narrow dispersion of proton chemical shifts is a strong indicator of an intrinsically disordered protein, compared to well-ordered proteins, which exhibit more broadly distributed peaks in the proton dimension (7). The triplet outliers, connected by horizontal lines, are signals from the side chains of glutamine residues in this sequence and are not an indication of local structure.

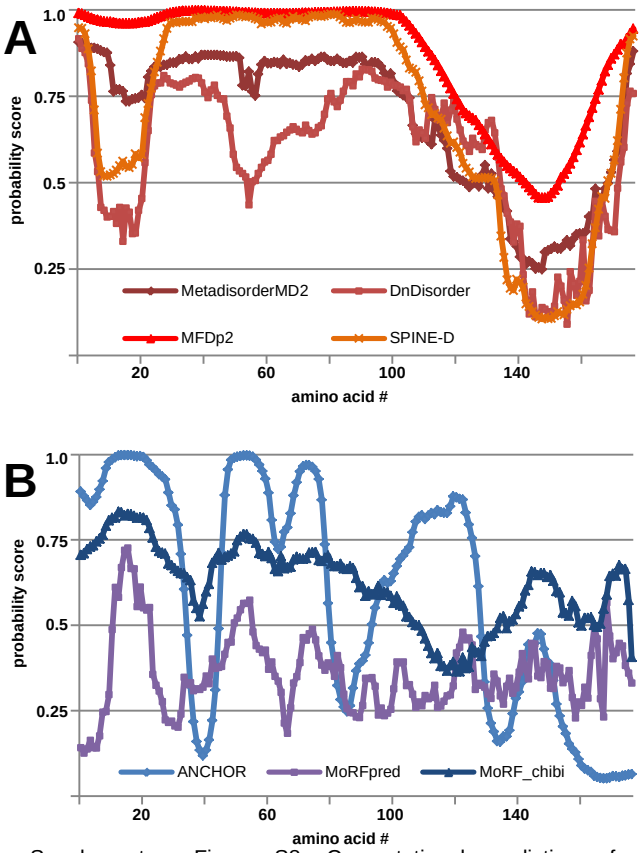

Supplementary Figure S8: Computational prediction of structural features in PopZ. (A) The propensity for intrinsic disorder, as indicated by four independent prediction programs: Metadisorder MD2 (8), DnDisorder (9), MFDp2 (10), and SPINE-D (11). (B) The presence of MoRF-like characteristics , as indicated by three independent prediction programs: ANCHOR (12), MoRFpred (13), and MoRFCHiBi_WEB (14). The combined average score for these programs is shown in Figure 5A of the main text.

1. Bowman GR, et al. (2010) Caulobacter PopZ forms a polar subdomain dictating sequential changes in pole composition and function. *Mol Microbiol* 76(1):173–189.

2. Radhakrishnan SK, Thanbichler M, Viollier PH. (2008) The dynamic interplay between a cell fate determinant and a lysozyme homolog drives the asymmetric division cycle of *Caulobacter crescentus*. *Genes Dev*. 22(2):212-25.

3. Thanbichler M, Iniesta AA, Shapiro L (2007) A comprehensive set of plasmids for vanillate- and xylose- inducible gene expression in *Caulobacter crescentus*. *Nucleic Acids Res*. 35(20).
4. Sliusarenko O, Heinritz J, Emonet T, and Jacobs-Wagner C (2011) High- throughput, subpixel-precision analysis of bacterial morphogenesis and intracellular spatio-temporal dynamics. *Mol. Micro*; 80(3):612-627.

5. Park DM, Jiao Y (2014) Modulation of medium pH by *Caulobacter crescentus* facilitates recovery from uranium-induced growth arrest. *Appl Environ Microbiol* 80(18):5680–5688.

6. Jacobs C, Domian IJ, Maddock JR, Shapiro L. (1999) Cell cycle-dependent polar localization of an essential bacterial histidine kinase that controls DNA replication and cell division. *Cell*. Apr 2;97(1):111-9

7. Dyson HJ, Wright PE (2004) Unfolded proteins and protein folding studied by NMR. *Chem Rev* 104(8):3607–3622.

8. Kozlowski LP, Bujnicki JM (2012) MetaDisorder: a meta-server for the prediction of intrinsic disorder in proteins. *BMC Bioinformatics* 13:111.

9. Eickholt J, Cheng J (2013) DNdisorder: predicting protein disorder using boosting and deep networks. *BMC Bioinformatics* 14:88.

10. Mizianty MJ, Uversky V, Kurgan L (2014) Prediction of intrinsic disorder in proteins using MFDp2. *Methods Mol Biol Clifton NJ* 1137:147–162.

11. Zhang T, et al. (2012) SPINE-D: accurate prediction of short and long disordered regions by a single neural-network based method. *J Biomol Struct Dyn* 29(4):799–813.

12. Dosztányi Z, Mészáros B, Simon I (2009) ANCHOR: web server for predicting protein binding regions in disordered proteins. *Bioinforma Oxf Engl* 25(20):2745–2746.

13. Disfani FM, et al. (2012) MoRFpred, a computational tool for sequence-based prediction and characterization of short disorder-to-order transitioning binding regions in proteins. *Bioinforma Oxf Engl* 28(12):i75–83.

14. Malhis N, Wong ETC, Nassar R, Gsponer J (2015) Computational Identification of MoRFs in Protein Sequences Using Hierarchical Application of Bayes Rule. *PloS One* 10(10):e0141603.